THE PUBLISHING HOUSE
OF THE ROMANIAN ACADEMY

PROCEEDINGS OF THE ROMANIAN ACADEMY, Series A,
Volume 27, Number 1/2026, pp. 69–78
DOI:

MECHANICAL BEHAVIOR AND ACOUSTIC EMISSION CHARACTERISTIC OF COAL-ROCK COMPOSITE WITH PREFABRICATED HOLE UNDER COMPRESSION

Ansen GAO[1, 2], Chengzhi QI[3], Kuan JIANG[4], Sunhao ZHENG[3], Yanjie FENG[5], Xiaoyu MA[3], Zhen WEI[6]

[1] Shandong University, School of Civil Engineering, Jinan 250061, China

[2] Shandong University, State Key Laboratory for Tunnel Engineering, Jinan 250061, China

[3] Beijing University of Civil Engineering and Architecture, School of Civil and Transportation Engineering, Beijing 100044, China

[4] Shandong University, School of Future Technology, Jinan 250061, China

[5] China University of Mining & Technology (Beijing), School of Mechanics and Civil Engineering, Beijing 100083, China

[6] Lanzhou Institute of Technology, School of Civil Engineering, Lanzhou 730050, China

Corresponding author: Ansen GAO, E-mail: gaoansen@163.com

Abstract. In deep coal mining, the stability of coal roadways is critically governed by its immediate roof and floor strata. This study investigated the evolution characteristics of mechanical behaviors of coal-rock composites, aiming to elucidate its failure mechanism. Results demonstrated that, compared to sandy mudstone-coal-sandy mudstone (SCS) composites, the red sandstone-coal-red sandstone (RCR) composites exhibited more pronounced fracturing, greater stress fluctuations, and significantly higher acoustic emission (AE) activities, characterized by markedly higher AE ringing counts. For SCS composites, AE ringing counts surged at the initial stress drop point, and peaked twice near its ultimate failure point. Notably, between these two points, a distinct quiescent phase of AE activities was identified, serving as a precursor for imminent failure. Furthermore, the generation of tensile and shear cracks exhibited both a spatiotemporal concentration and a distinct stage-dependent evolution pattern. Specifically, AE events in SCS composites were concentrated vertically with higher density within the central coal layer, while in RCR composites, the high-energy AE events clustered predominantly at the mid-height region. Ultimately, both SCS and RCR composites failed through transverse dilatancy, characterized by the localization of macroscopic fractures within the central coal block. These findings provide crucial insights for the early-warning strategies of coalbursts hazards in deep coal mines.

Keywords: mechanical behavior, AE characteristic, coal-rock composite, prefabricated hole, compression

1. INTRODUCTION

As shallow coal resources became exhausted, coal mining progressively transitioned to deeper strata [1-2]. With increasing depth, both the frequency and intensity of coalbursts surged, posing significant threats

to mine safety and production [3]. In deep roadways, coal and rock typically exist not as isolated entities but as mechanically interactive coal-rock composites, forming a composite system [4-5]. Consequently, the triggering mechanisms of these dynamic failures were related not only to the mechanical properties of coal, but also to those of the adjacent rock. Therefore, studying the mechanical behaviors of coal-rock composites is crucial for understanding deep roadway dynamic disasters. Coal-rock composites generally exhibited marked transverse isotropy, so that their deformation and strength were significantly different from those of homogeneous rock masses. The multi-scale defects, including cracks and pores inherent in coal and rock, fundamentally govern the complexity of their strength evolution and instability behaviors.

Previous studies extensively explored the influence of prefabricated cavity geometries on rock's strength and fracture. Li et al. demonstrated that hole size, shape and inclination significantly impacted marble strength [6], while Zhou et al. found cavity number and layout crucially affected the mechanical behavior of flaws in marble [7]. Yang et al. established that angles between coplanar flaws-controlled the fracture processes of sandstone [8]. Zhao et al. studied the characteristic cracks patterns around cylindrical cavities in granite under compression [9]. They observed tensile cracks at the roof and floor, compressive slabbing (spalling) on the sidewalls, and secondary remote cracks. These crack types corresponded to the primary tensile, compressive slabbing, and remote fracture types identified by Carter et al. [10], all of which propagated parallel to the direction of maximum compression. The initiation location of cracks was found to depend on cavity size and confinement conditions. However, these studies primarily focused on the fundamental failure mechanisms. Their understanding of more complex aspects remained limited, particularly regarding interactive effects, sequential crack evolution, lithological influences, and detailed failure mechanics. Ma et al. analyzed coal-rock composites with inclined cracks using PFC and AE method but did not elucidate the sequential evolution or source locations of derived cracks [11]. Ma et al. identified how spherical defect size and position reduced strength and dictated failure modes (tensile, shear, mixed), yet analyses were confined to single-lithology samples, omitting multi-lithology responses [12]. Liu et al. observed holes prolonged compaction, reduced AE activity, and characterized tensile and shear cracks distributions, but did not reveal the underlying failure mechanics or temporal cracks sequence [13]. Gao et al. modeled coal ejection preceding rockburst in composites [14], highlighting tensile cracks but lacking a prefabricated hole in the coal, limiting direct applicability to deep roadways. Xin et al. compared fracture evolution around tunnels of different shapes [15]. They found that rectangular tunnels offered better resistance to rockburst. However, their study did not analyze the influence of lithology or the temporal evolution of cracks. Meng et al. documented that tensile cracks initiated at large double pores, leading to brittle failure [16]. Yet, their work provided limited detail on the distribution of fracture types across different stages of failure.

Consequently, most earlier investigations of coalburst concentrated on the failure responses of individual coal or rock materials, their conclusions did not fully represent the failure mechanism of the typical coal-rock composite geological structure. Therefore, by experimental research and numerical simulation analysis, we studied the mechanical behavior and AE characteristic of coal-rock composites with prefabricated round hole under uniaxial compression. These results can provide a new method to evaluate the failure-instability state of coal-rock composites, and it also has certain reference significances for the prevention and control of coal-rock dynamic disasters in deep underground engineering.

2. EXPERIMENTAL PROCEDURES

The Instron 5985 universal testing machine was used to perform compression tests in this experiment. AE signals were acquired using the PCI-II data acquisition system. A total of six sensors were installed on the specimen, with three sensors on the upper block (both side surfaces and the rear surface) and three sensors on the lower block (both side surfaces and the front surface). The upper and lower sensor groups were positioned on two horizontal planes, with all sensors installed at the center of their respective surfaces. The upper sensor plane was 2 cm from the top of the specimen, and the lower sensor plane was 2 cm from the bottom of the specimen. The operating frequency range of the sensors used was 125–750 kHz, with a resonant frequency of 300 kHz. The sampling frequency for signal acquisition was set to 1 MHz, the threshold voltage was 100 mV, the detection threshold was 45 dB, and the preamplifier gain was 40 dB. During the acquisition process of AE signals, the threshold and gain settings were configured to ensure a high signal-to-noise ratio. Raw signals were filtered to further suppress noise. Acoustic emission event localization was performed using an algorithm based on the time difference of arrival (TDOA) method, which solves a nonlinear optimization problem to determine the spatial coordinates and onset time of the events.

Red sandstone cuboid blocks (5 cm × 5 cm × 3 cm) and coal cuboid blocks (5 cm × 5 cm × 4 cm) were bonded to form red sandstone-coal-red sandstone composites (Fig. 1b), and sub-figures (b) among all the pictures below. Similarly, sandy mudstone blocks (5 cm × 5 cm × 3 cm) and coal blocks (5 cm × 5 cm × 4 cm) were assembled into sandy mudstone-coal-sandy mudstone composites (Fig. 1a), and sub-figures (a) among all the pictures below. All rock and coal blocks were cemented using structural adhesive. All specimens originated from the same parent rocks. Prior to testing, a 1 cm diameter round hole, penetrating completely through the coal section, was machined in each coal specimen, and the displacement-controlled loading at a rate of 0.1 mm/min was applied throughout the experiment.

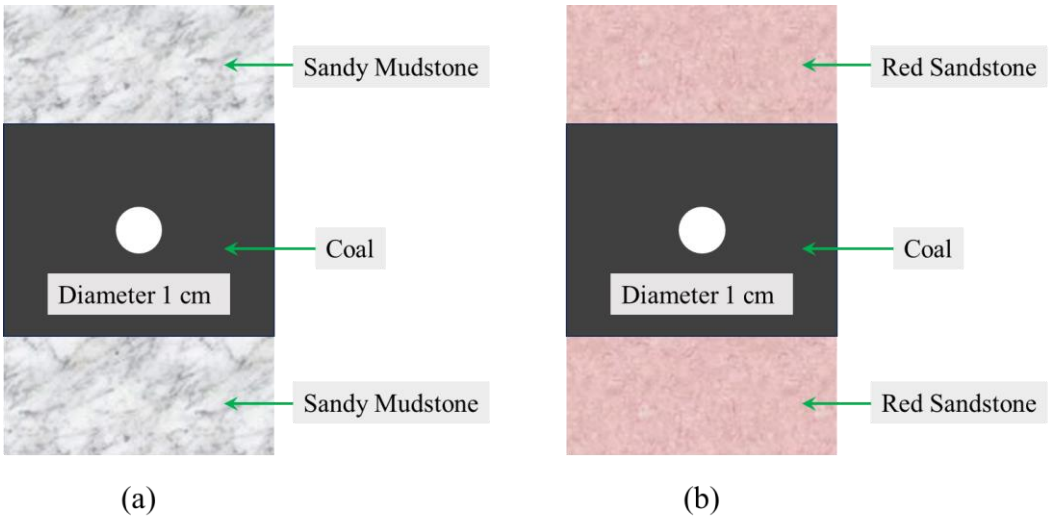

Fig. 1 Schematic diagram of the SCS composite and RCR composite

3. RESULTS

3.1 Stress and AE Response Characteristics of Coal-Rock Composite with Prefabricated Hole under Compression

The stress curves for both sandy mudstone-coal-sandy mudstone and red sandstone-coal-red sandstone composites exhibited three distinct stages (Fig. 2): stage I (compaction), characterized by a downward-convex shape indicating initial crack closure; stage II (elastic deformation), featuring near-linear stress increase with minor initial stress fluctuations/drops until the yield point; stage III (critical failure), showing significant stress fluctuations and multiple minor drops prior to ultimate failure, suggesting a transition towards elastoplastic failure. Then, for sandy mudstone composites, AE signals displayed low and minimally fluctuating counts during stages I and II. This indicated limited micro-fracturing and small energy releases. These results were consistent with the synchronous mechanical responses of the composites.

In Stage III, AE ringing counts surged significantly and became highly variable, coinciding with the initial stress drop and immediately preceding final failure. A relatively calm period was observed between these surges, potentially serving as a failure precursor. Then, the RCR composites demonstrated markedly higher and more variable AE activity from Stage I onwards, indicating more intense micro-fracturing and larger energy releases, corresponding to more severe fragmentation. This pronounced early AE activity, reflecting the high failure strength contrast, concentrated micro-fracturing within the weaker coal from the onset, and it generated substantial elastic stress waves, driving strong AE fluctuations even prior to the yield point.

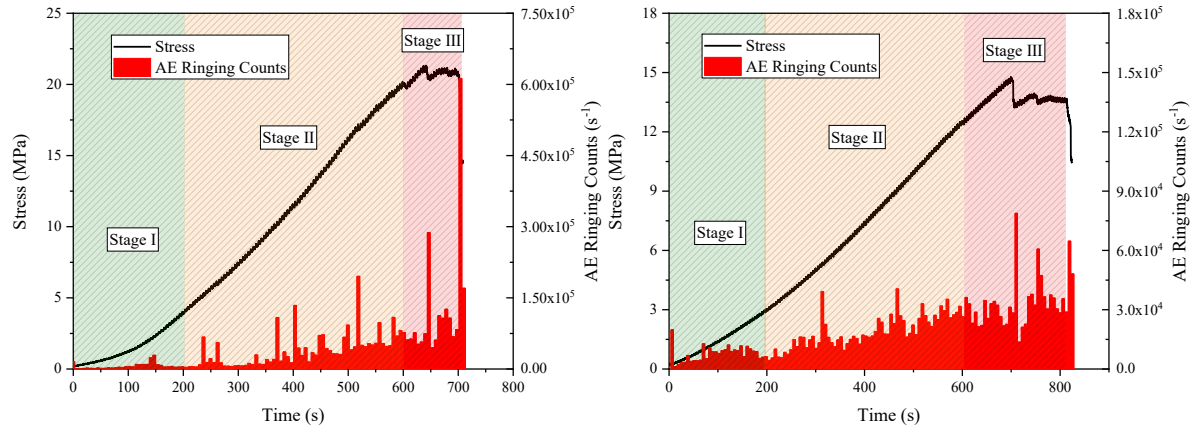

Fig. 2 Evolution characteristics of AE ring counts for coal-rock composite with prefabricated hole under compression

3.2. Evolution Characteristic of Cracks of Coal-Rock Composite with Prefabricated Hole under Compression

Average Frequency (AF) and Risetime Amplitude (RA) are commonly used acoustic emission parameters for identifying crack types of rocks during its fracture-instability processes. Specifically, AF reflects the frequency of acoustic emission events per unit time, calculated as the ratio of the ring-down count to the waveform duration. RA is the ratio of the rise time to the peak amplitude. Based on previous established methods [17-19], the relationship between AF and RA can be utilized to distinguish crack types, that data points located above the RA-AF diagonal typically correspond to tensile cracks, whereas points below the diagonal indicate shear cracks. Then, we defined the fracture type coefficient k, for k = AF/RA, to characterize the evolution characteristics of different fracture types of rocks. It should be further explained that $k > 1$ represented tensile fractures, and $k < 1$ represented shear fractures. To illustrate, the value of coefficient k only represented fracture types, it cannot represent the failure intensity of rocks.

For SCS composite (Fig. 3a), the generation of cracks had a certain concentration phenomenon in time, its fracture behavior was mainly concentrated in 400-600 s, which corresponded to the stress fluctuation response of rocks. Therefore, we can confirm that it is accurate and reliable to characterize tensile cracks and shear cracks by the parameter *k*. Corresponding to RCR composite (Fig. 3b), the tensile and shear fracture behaviors had certain stage characteristics. It showed that the occurrence of tensile and shear cracks of red sandstone-coal composite has certain sequential and stage characteristics, its fracture behaviors appeared at about 320 s, 460 s, 650 s and 700 s.

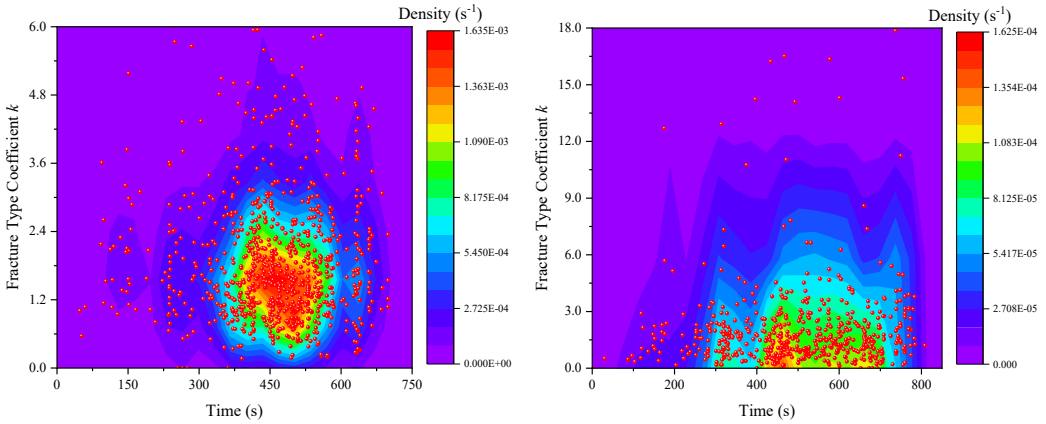

Fig. 3 Evolution characteristics of tensile and shear cracks for coal-rock composite under compression

3.3 AE Events and Macroscopic Fracture of Coal-Rock Composite with Prefabricated Hole under Compression

As illustrated in Fig. 4, AE events in sandy mudstone-coal composite exhibited a distinct longitudinal distribution zone, with higher event density concentrated in the central coal block. For red sandstone-coal composite, AE events clustered predominantly at the mid-height region, where high-energy events were particularly localized. Macroscopic fractures consistently localized within the central coal block for both composites, accompanied by transverse dilatational fracturing. Minor longitudinal cracks and limited small-scale fracturing occurred in the upper and lower sandy mudstone sections. For red sandstone composite, severe failure preferentially developed within the lower-strength coal block. These results indicated that a significant strength difference of coal and rock materials was the primary condition for coalbursts in deep roadways, with mining-induced stresses acting as the driving force.

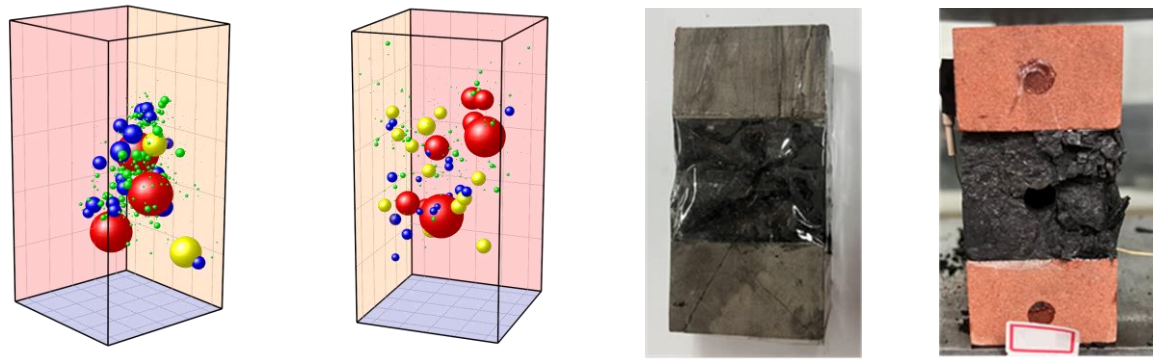

Fig. 4 AE events and macroscopic failure characteristics of coal-rock composite with prefabricated hole under compression

3.4 Numerical Simulation of Failure-Instability of Coal-Rock Composite with Prefabricated Hole under Compression

The Particle Flow Code (PFC) simulations of uniaxial compression tests on coal-rock composites were used to replicate laboratory test (Fig. 5). The force chain analysis revealed densely packed compressive (red color and square dashed box in Fig. 5) chains dominating the sandy mudstone layers, indicating strong load-bearing capacity and uniform stress distribution, while the coal seam exhibited sparse chains with tensile (blue color and square dashed box in Fig. 5) components, reflecting its lower strength and tensile failure susceptibility. The force chains transferred preferentially from rock to coal, concentrating stress at interfaces. The pattern of cracks were predominantly tensile cracks (green color and elliptical dashed box), concentrating around prefabricated pores, and radiating outward in an X-shaped pattern from central pores, highlighting pore-induced tensile stress concentration. The shear cracks (yellow color and elliptical dashed box) were fewer and localized near holes (RCR composite in Fig. 5a) and coal block edges (SCS composite in Fig. 5b), indicating shear stress concentrations. Then, the compressive chains concentrated within the primary fracture zone, aligning with its direction. Crucially, the tensile cracks propagated preferentially along the weak coal interlayer. They linked the tips of pores to form through-going cracks. This identified the interlayer as the initiation point of failure, a process that was accelerated by the presence of prefabricated holes. The results demonstrated that it occurred a tension-shear composite failure mode, which governed by material heterogeneity, pore presence and loading conditions.

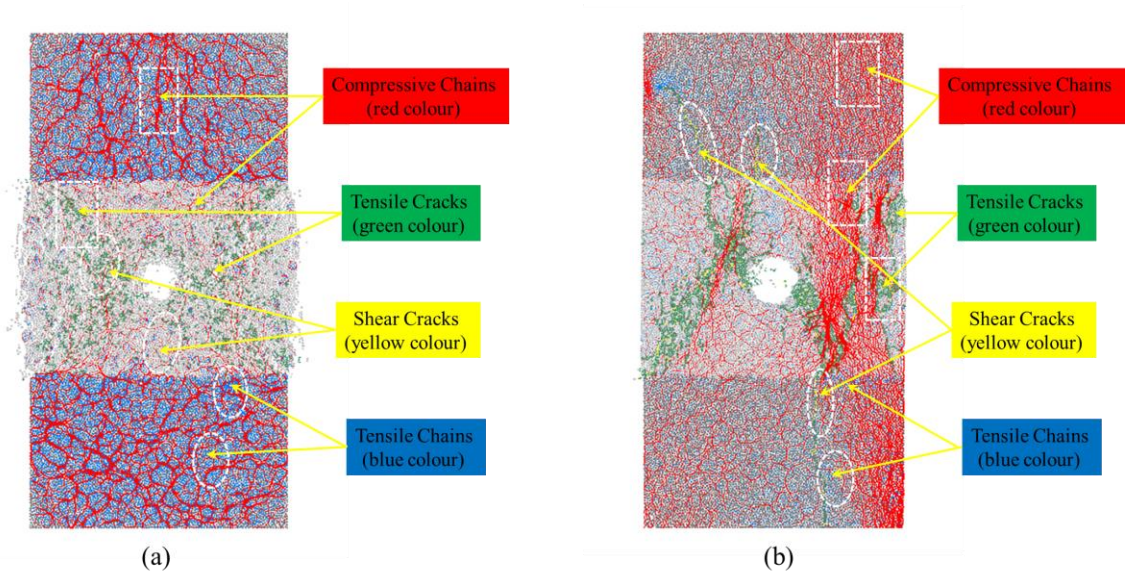

Fig. 5 Numerically simulation results of force chain and cracks of coal-rock composite under compression

4. DISCUSSION

The results indicated that there existed a significant difference of the failure behaviors between two different lithological composites (RCR composite and SCS composite). This was primarily influenced by differences in their macroscopic failure modes, cracks evolution pattern, and energy release responses. The RCR composite exhibited typical dynamic response characteristics, where under high stress, the high-strength red sandstone accumulated substantial elastic strain energy, while the relatively weak coal interlayer

became the outlet for stress release. Its failure was dominated by transverse tensile splitting of the coal layer, leading to intense lateral expansion and bursting of the specimen. This corresponded to dense high-energy AE events and a massive total energy release. In contrast, the SCS composite presented the characteristics of relatively static failure mode. The strength difference between the sandy mudstone and coal was relatively small, with failure manifesting as a shear slip band developing longitudinally along the composite. And then, cracks were concentrated in the middle of the coal interlayer, the failure process was more progressive, and the resulting fragments were larger. The corresponding AE activity was generally weaker. This comparison of macroscopic failure modes clearly indicated that a higher strength contrast between the rock layers was a critical condition for inducing more intense and impact-prone failure.

This study also found that a relative quiet period of AE activity existed before the final instability of the specimens. This phenomenon was related to stable cracks propagation and local stress redistribution, which supported previous observational findings in research on precursors to rock failure [20-22]. However, the results of this study provided new insights and additions regarding the controlling mode of the fracture path leading to specimen instability. For the heterogeneous lithological composites, although the prefabricated hole still initiated the initial cracks, their subsequent propagation paths were strongly controlled by lithological interfaces and strength contrasts. For instance, in RCR composite, although the cracks originated from the hole, they quickly turned and propagated along the weak coal interlayer, establishing a dominance of transverse tensile splitting. In SCS composite, cracks propagation was more controlled by the overall shear band rather than being solely guided by the hole.

Moreover, compared to SCS composite, the RCR composite exhibited high AF values and low RA values during the early stage of failure. In this case, $k > 1$ corresponded to a tensile fracture mechanism, which explained its failure mode dominated by transverse tensile splitting. The presence of the prefabricated hole led to strong tensile stress concentration around it during the initial loading stage of the specimen. This directly induced the initiation of the first batch of tensile microcracks, manifested as the initial spatial clustering of AE events around the hole. As the load increased, the propagation direction of these initial cracks was no longer determined solely by the hole structure, and it was governed by the drive towards the path of minimum energy release from the hard rock layer to the weak coal layer. This resulted in the macroscopic fractures primarily located within the weakest coal interlayer. Therefore, the composite of high-strength surrounding rock and a weak coal layer constitutes a high-risk composite system, characterized by failure driven by the instantaneous release of elastic strain energy through tensile bursting. In contrast, composites with similar strengths present lower risk, with failure characterized by shear slip and progressive damage.

This study investigated the differences of mechanical responses of composite specimens with different lithological combinations. Some of the conclusions corroborate findings from previous experimental explorations [11, 23] and theoretical understandings [12, 24-25]. However, the small-scale specimens, the limited types of lithological combinations, and the simplified loading conditions make it difficult to fully replicate the true in situ stress conditions encountered in underground engineering. Nevertheless, the fundamental laws governing the mechanical response of composite specimens during its failure and instability process, as revealed in this study, can still provide an important basis for a deeper understanding of the stability of surrounding rock in deep engineering and the mechanisms of coalburst.

5. CONCLUSION

Based on the integrated methodologies of acoustic emission monitoring, uniaxial compression tests, and numerical simulation, this study conducted a comparative experimental investigation into the mechanical response of failure-instability processes of SCS composites and RCR composites. The main conclusions are as follows:

(1) Compared to SCS composites, the RCR composites exhibited more significant fracture responses during its failure-instability process, with intensified stress fluctuations and dramatic increases of AE ringing counts. In both types, AE ringing counts displayed volatile growth curves after entering the critical stage, surging near its stress drop points. A distinct calm period of AE activity occurred between initial stress drops and final instability points, establishing this phenomenon as a reliable failure precursor.

(2) The generation of tensile and shear cracks showed temporal concentration and staged evolution, correlating directly with stress-increase responses. This correspondence confirmed fracture type coefficient k could effectively characterize cracks evolution patterns during rock failure process.

(3) AE events in SCS composites formed a longitudinal distribution zone with higher density concentrated in the middle coal layer. The RCR composites exhibited centralized AE events in the composite's core, where high-energy events clustered densely. Transverse expansion fractures consistently localized in the coal interlayer, demonstrating that macroscopic failure preferentially occurs in low-strength coal blocks.

Through laboratory-scale experiments on small-sized specimens, this study revealed the key controlling effect of lithological differences on the instability and failure behavior of coal-rock composites. However, it should be noted that the conclusions are based on specimens of a specific size (5 cm × 5 cm × 10 cm) and simplified loading conditions (uniaxial compression), and do not fully account for the combined influence of factors such as the three-dimensional stress state, scale effects, and groundwater present in real geological environments. Furthermore, the current work primarily focuses on two typical lithological combinations (RCR composite and SCS composite), and the generalizability of the conclusions requires further validation through experiments on more lithological combinations.

Therefore, our future study work needs to be further deepened and refined. Specifically, large-scale physical model tests can be conducted to investigate the influence of scale effects on the failure and instability modes of the composite bodies. Meanwhile, comparative experiments on different lithological combinations under true triaxial loading can be carried out to more closely approximate actual engineering stress conditions, thereby obtaining more realistic failure and instability mechanisms of coal-rock composites. This will provide a more reliable practical basis for risk assessment of deep engineering hazards.

ACKNOWLEDGEMENTS

This study was supported by the Youth Foundation of Shandong Natural Science Foundation of China (Grant No. ZR2025QC469), the National Natural Science Foundation of China (Grant No. 52438007 and No. 12172036), the Gansu Provincial Young Doctor Program (Grant No. 2024QB-103), the Gansu Provincial Youth Science and Technology Foundation (Grant No. 24JRRA1012), the Lanzhou Young Scientific and Technological Talents Innovation Project (Grant No. 2024-QN-74).

REFERENCES

[1] Kang H, Gao F, Xu G, Ren H. Mechanical behaviors of coal measures and ground control technologies for China's deep coal mines-A review. J Rock Mech Geotech 2023;15(1):37-65. Doi:10.1016/j.jrmge.2022.11.004.

[2] Ranjith PG, Zhao J, Ju M, De Silva RV, Rathnaweera TD, Bandara AK. Opportunities and challenges in deep mining: a brief review. Engineering 2017;3(4):546-551. Doi:10.1016/J.ENG.2017.04.024.

[3] Zhang J, Jiang F, Yang J, Bai W, Zhang L. Rockburst mechanism in soft coal seam within deep coal mines. Int J Min Sci Techno 2017;27(3):551-556. Doi:10.1016/j.ijmst.2017.03.011.

[4] Cai W, Dou L, Si G, Cao A, Gong S, Wang G, Yuan S. A new seismic-based strain energy methodology for coal burst forecasting in underground coal mines. Int J Rock Mecha Min 2019;123:104086. Doi:10.1016/j.ijrmms.2019.104086.

[5] Mark C, Gauna M. Evaluating the risk of coal bursts in underground coal mines. Int J Min Sci Techno 2016;26(1):47-52. Doi:10.1016/j.ijmst.2015.11.009.

[6] Li D, Zhu Q, Zhou Z, Li X, Ranjith PG. Fracture analysis of marble specimens with a hole under uniaxial compression by digital image correlation. Eng Fract Mech 2017;183:109-124. Doi:10.1016/j.engfracmech.2017.05.035 .

[7] Zhou Z, Tan L, Cao W, Zhou Z, Cai X. Fracture evolution and failure behaviour of marble specimens containing rectangular cavities under uniaxial loading. Eng Fract Mech 2017;184:183-201. Doi:10.1016/j.engfracmech.2017.08.029.

[8] Yang SQ, Huang YH, Tian WL, Zhu JB. An experimental investigation on strength, deformation and crack evolution behavior of sandstone containing two oval flaws under uniaxial compression. Eng Geol 2017;217:35-48. Doi:10.1016/j.enggeo.2016.12.004.

[9] Zhao XD, Zhang HX, Zhu WC. Fracture evolution around pre-existing cylindrical cavities in brittle rocks under uniaxial compression. T Nonferr Metal Soc 2014;24(3):806-815. Doi:10.1016/S1003-6326(14)63129-0.

[10] Carter BJ, Lajtai EZ, Yuan Y. Tensile fracture from circular cavities loaded in compression. Int J Fract 1992;57:221-236. Doi:10.1007/BF00035074.

[11] Ma S, Liu K, Guo T, Yang J, Li X, Yan Z. Experimental and numerical investigation on the mechanical characteristics and failure mechanism of cracked coal & rock-like combined sample under uniaxial compression. Theor Appl Fract Mec 2022;122:103583. Doi:10.1016/j.tafmec.2022.103583.

[12] Ma W, Cui C, Li X. Mechanical responses and stress distribution of rock-like specimen containing a spherical defect under uniaxial compression. Theor Appl Fract Mec 2024;130:104251. Doi:10.1016/j.tafmec.2023.104251.

[13] Liu X, Zhang H, Wang X, Zhang C, Xie H, Yang S, Lu W. Acoustic emission characteristics of graded loading intact and holey rock samples during the damage and failure process. Applied Sciences 2019;9(8):1595. Doi:10.3390/app9081595.

[14] Gao F, Kang H, Yang L. An experimental investigation into the strainburst process under quasi-static loading. Rock Mech Rock Eng 2020;53(12):5617-5629. Doi:10.1007/s00603-020-02231-y.

[15] Xin J, Jiang Q, Li S, Chen P, Zhao H. Fracturing and energy evolution of rock around prefabricated rectangular and circular tunnels under shearing load: A comparative analysis. Rock Mech Rock Eng 2023;56(12):9057-9084. Doi:10.1007/s00603-023-03532-8.

[16] Meng F, Wen Z, Shen B, Jing S, Welgama PD, Huang J. Fracture and evolution characteristics of specimens containing double holes. Geomech Eng 2021;26(6):593-605. Doi:10.12989/gae.2021.26.6.593.

[17] Aggelis DG. Classification of cracking mode in concrete by acoustic emission parameters. Mech Res Commun 2011;38(3):153-157. Doi:10.1016/j.mechrescom.2011.03.007.

[18] ElBatanouny MK, Larosche A, Mazzoleni P, Ziehl PH, Matta F, Zappa E. Identification of cracking mechanisms in scaled FRP reinforced concrete beams using acoustic emission. Exp Mech 2014;54:69-82. Doi:10.1007/s11340-012-9692-3.

[19] Elfergani HA, Pullin R, Holford KM. Damage assessment of corrosion in prestressed concrete by acoustic emission. Constr

Build Mater 2013;40:925-933. Doi:10.1016/j.conbuildmat.2012.11.071.

[20] Su G, Huang L, Qin Y, Yan X. Experimental study of the “AE quiet period” on the eve of brittle failure in hard rock. Eng Fail Anal 2024;162:108391. Doi:10.1016/j.engfailanal.2024.108391.

[21] He S, Qin M, Qiu L, Song D, Zhang X. Early warning of coal dynamic disaster by precursor of AE and EMR “quiet period”. Int J Coal Sci Techn 2022;9(1):46. Doi:10.1007/s40789-022-00514-z.

[22] Wang CL, Zhou BK, Li CF, Wen ZJ, Bai ZA, Zhu CY, Sun L, Xue XH, Cao P. Prediction and critical transition mechanism for granite fracture: Insights from critical slowing down theory. J Cent South Univ 2024;31(8):2748-2764. Doi:10.1007/s11771-024-5707-3.

[23] Yuan A, Hou J, Yin Z. The force chain and acoustic emission response law for the uniaxial compression of rock. Geotech Geol Eng 2020;38:4479-4499. Doi:10.1007/s10706-020-01303-8.

[24] Zhang C, Canbulat I, Hebblewhite B, Ward CR. Assessing coal burst phenomena in mining and insights into directions for future research. Int J Coal Geol 2017;179:28-44. Doi:10.1016/j.coal.2017.05.011.

[25] Hu S, Zhou X, Ru W, Han J, Guo S, Zhang C, Yang L. Study on mechanical property of coal-rock combination under different unloading confining pressure rate. Geotech Geol Eng 2023;41(4):2629-2644. Doi:10.1007/s10706-023-02417-5.

Received September 4, 2025